Chapter 5   Particulates

5.1   Introduction

Emissions of ash and other solid particles from power plants and other industrial activities were the first that called for action. There are several reasons for that. First, since down to a size of a few micron particles (or droplets) can be seen by the naked eye, the problems could not have remained unnoticed. Secondly, the emissions produce a hazard much closer to the source than gaseous pollutants do: material is deposited within a shorter range. As a first response to this, high stacks have been erected worldwide. A third reason is that the amount of dust that may be emitted from, for example, a coal-fired power plant, per unit output power is much higher than for other pollutants. This is simply because the amount of ash-forming material in coals is much larger than the amount of sulphur, nitrogen *etc.*, being typically 10-20 %-wt (dry). This, in combination with the fact that large-scale use of coal as an energy source was about fifty years ahead of oil and gas explains why dust emissions from coal-fired power plants have been controlled since the 1920s (☞ chapter 2). Electrostatic precipitators or ESPs (∟ section 5.7), still a leading technology in this field, were applied for this purpose almost exclusively in these days: efficiencies have increased from ~ 90% to ~ 99% since then (Klingspor and Vernon, 1988).

During the last decades the maximum allowable emissions of particulates have decreased, for coal firing in western Europe, from 150 - 200 mg/m^3_{STP} in the 1980s to typically 50 mg/m^3_{STP} in the 1990s, with 20 mg/m^3_{STP} as the limit for the near future for units larger than 300 - 500 $MW_{thermal}$. Although the environment and health-related issues are the most important motivations for the control of particulate emissions several other factors contribute to the picture. As the other chapters demonstrate, other pollutants have to be controlled as well and the technologies applied for that do not allow for high loads of fly ash or other condensed matter in the gas to be treated. More recently, the coming-of-age of integrated processes based on pressurised fluidised bed combustion and coal gasification with combined cycle power generation (PFBC-CC and IGCC) presented the problem of hot (and pressurised) gas clean-up for dust. Modern expansion turbines applied there do not allow for turbine inlet dust concentrations higher than a few ppmw, with additional requirements for particles larger than 10 μm and 2 μm. This maximum dust load is less than $1/10^{th}$ of a typical allowable emission to the environment (Stringer and

Meadowcroft, 1990, Mitchell, 1997).

Two other reasons for dust control measures are not specific for power plants or energy-related processes: in some processes the "dust" is in fact a (valuable) product or an expensive catalyst, whilst in all cases the risk for dust explosions is reduced when particulates are not left uncontrolled.

Fuels do not contain ash as such. During combustion or gasification inorganic mineral impurities in fuels are converted into solid, liquid and gaseous compounds, which finally leave the system as bottom ashes, fly ashes or vapour. Due to condensation and other processes some vapours solidify, whilst others may pass the entire emissions control system and leave via the stack. An example for the latter is mercury (Hg), of which 50% or more of the input is emitted to the environment (⌐ chapter 8). For a generalised pulverised coal combustion system (dry bottom firing, with an ESP for dust control and conventional wet FGD, ↗ chapter 3), a typical distribution of ashes and other solid residues streams is given in Figure 5.1
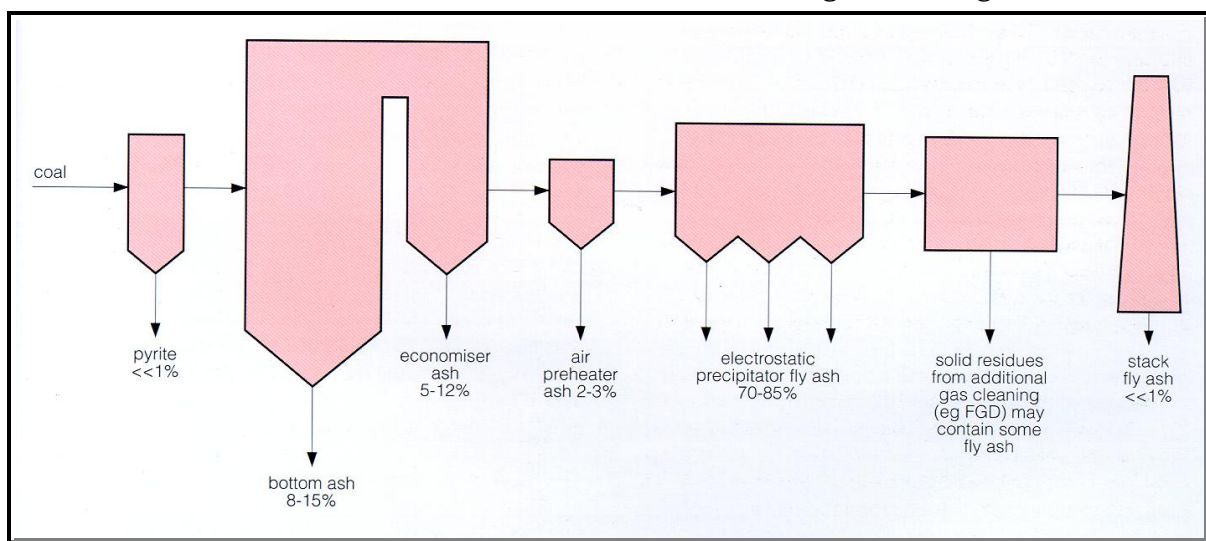

Figure 5.1   Typical distribution of ashes and solid residues streams from a general pulverised coal combustion unit (picture from Carpenter, 1998)

Into what form the ash-forming material will finally be converted depends on many factors, such as temperature, surrounding gas atmosphere (combustion or gasification), pressure, fuel particle size, fuel particle size distribution, residence time, *etc.*, some of which are dictated by process type and furnace design. It must be noted that for solid fuel-based processes the furnace design is to a very large extent pre-determined by how the ashes are expected to behave inside the unit and how and where to remove them, as bottom ashes or fly ashes. Many operation and maintenance problems with solid fuel-fired systems are related to the behaviour of

the ashes, both during and after their formation. Most important here is deterioration of system components by corrosion *etc.* and water-tube failures that eventually enforce a total system shut-down. An extensive overview of the effects of ash-forming components on furnace and boiler operation was given not too long ago by Bryers (1996) for fossil fuels, biomass and waste-derived fuels.

Knowledge and understanding of ash-related issues in relation to combustion and gasification processes is largely based on a long experience with coal and peat. With these fuels the ashes formed are mainly composed of oxides of silicon, aluminum and iron (SiO_2, Al_2O_3 and Fe_2O_3). Small amounts of alkali metals present are bound to sulphates since an excess amount of sulphur is introduced with the fuel as well. This general knowledge is of limited use when considering the alternative, renewable fuels that currently penetrate the energy market, such as biomass and waste-derived fuels. Despite the fact that biomass contains very little ash (typically less than 0.5 %-wt dry), the chemical characteristics of these "new" fuels makes them rather troublesome in comparison with coal. High levels of potassium and often also chlorine, in combination with a sulphur content near zero have presented a completely new set of problems related to boiler and furnace operation and maintenance.

A feature of ashes and particulate solids in general is that they possess a particle size distribution and have a certain shape that may be close to spherical or far from that. For a general dry bottom pulverised coal combustion unit typical particle size distributions of bottom ashes and fly ashes as captured by the ESP are shown in Figure 5.2. Note that the incoming fuel particle size is typically 90%-wt below 100 µm for pulverised coal firing. Figure 5.2 gives a volume based distribution which is closely related to a mass distribution. Alternatively a number, length (diameter), or surface distribution can be used, depending on the measurement technique that is applied.
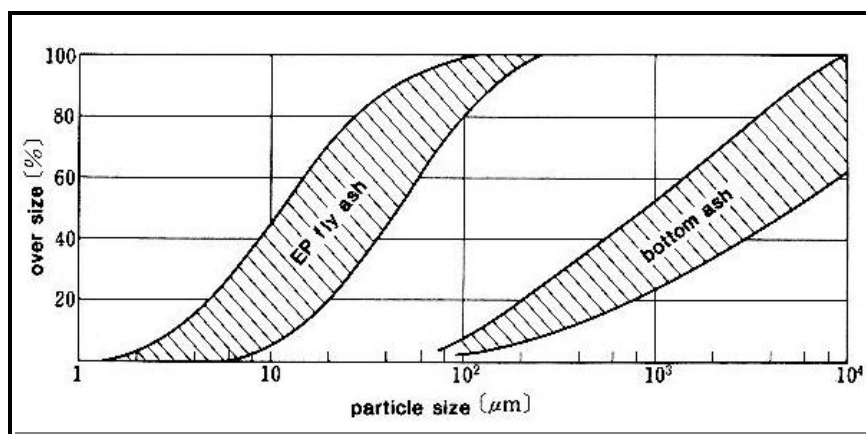

Figure 5.2   Typical volume-based cumulative size distributions for pulverised coal combustion fly ash and bottom ash. EP = electrostatic precipitator (picture from Iinoya *et al.*, 1991)

For modelling purposes log-normal, Rosin-Rammler-Sperling or Gates-Gaudin-Schumann distributions are

generally used, all three based on two statistical parameters. The non-spherical shape of a particle can be quantified by a single quantity such as the (Wadell) sphericity, ψ, using a perfect sphere as a reference:

$$\psi = 4.836 \frac{(\text{ volume of particle })^{\frac{2}{3}}}{\text{surface of particle}} = \frac{\text{surface of sphere with same volume}}{\text{surface of particle}} \qquad (5\text{-}1)$$

For a spherical particle, $\psi = 1$, for a cube $\psi = 0.81$, for coal powder $\psi = 0.65\text{-}0.75$ (Kunii and Levenspiel, 1991).

It is obvious that the removal of particles or droplets from a gas requires some understanding of what is generally known as "aerosol technology". Some of that will be mixed into this chapter. An aerosol is a suspension of solid or liquid particles in a gas, with particle sizes ranging from 0.001 to over 100 μm (Hinds, 1982). More details on solids handling, aerosols and particle technology in general can be found elsewhere (Iinoya *et al.*, 1991, Hinds, 1982, Zevenhoven and Heiskanen, 2000).

Considering the health risks presented by dust emissions from power plants the classifications PM_{10} (particulate matter finer than 10 μm) and $PM_{2.5}$ (particulate matter finer than 2.5 μm) are widely used. The $PM_{2.5}$ standard for ambient air quality was presented in 1997 by the US EPA as an addition to the PM_{10} standard, recognising that the differences in chemical composition and physical behaviour make the two size classes very different from an environmental impact and health hazard point of view. For Europe, a standard for $PM_{2.5}$ has been proposed for 2005 (Sloss and Smith, 1998). $PM_{2.5}$ class particles are a problem for the human respiratory system. The nose/mouth/throat system can't prevent the particles from entering the lungs; they can't be removed from lung tissue by the blood circulation either.

PM_{10} and $PM_{2.5}$ particulate matter as generated by human activities may be of the same order as what is produced by natural processes (sand and soil dispersion, sea salt, volcanoes). It is estimated that ⅓ of the PM_{10} comes from coal combustion, road transport is considered to be a more serious pollutant (diesel engines, leaded gasoline). In the US, 45% of $PM_{2.5}$ is connected to fossil fuel combustion. For a coal fired unit with ESP or baghouse filter the emissions will be in the finer PM_{10} range, being of the order $PM_{3.5}$ when a wet FGD scrubber is present, approaching $PM_{1.0}$ for the most efficient plant (Sloss and Smith 1998). One feature of $PM_{2.5}$ is that significant amounts of it are formed as so-called secondary particles. Sulphate and nitrate aerosols are produced by processes taking place in the atmosphere, whilst fragmentation of PM_{10}

particles adds to the $PM_{2.5}$ fraction as well. Clearly the problem goes far beyond controlling PM_{10} and $PM_{2.5}$ emissions from combustion and gasification facilities.

In this chapter the various methods to remove particulate matter, mainly fly ash, from combustion flue gases and gasification product gases will be dealt with. Following a short analysis of how ashes are generated and how they are correlated with ash-forming matter in the fuel, some emission standards for fly ash emissions are given. Starting with the largest particle size fraction, gravity settling and gas cyclones are discussed first. This is followed by the two most important technologies, being electrostatic precipitation (ESP), and baghouse/barrier filters, respectively. Then a short discussion on wet scrubbing is presented. After that the special problem of high temperature, higher pressure (HTHP) gas clean-up for particles is addressed. The chapter ends with a few words on particulate emissions from vehicles.

It is noted that organic particulate emissions such as tar and soot are not included in this chapter (⌐ chapter 6).

5.2   Ash-forming elements in fuels

As stated above, fuels do not contain ash as such. Apart from the combustible hydrocarbon part many inorganic mineral impurities are integrated within or mixed with the fuel: upon combustion or gasification this material will be oxidised to by-products of the process. Often this material can be put to further use, as is the case with fly ashes collected from the flue gas of a pulverised coal combustion facility (Sloss and Smith, 1996).

Geologically old fossil fuels contain highly integrated ash-forming matter. For low-grade coals and lignites a significant amount of that can be removed before further processing. Especially for steel processing application it is necessary to reduce the amount of ash-forming material ("coal washing"), or when the amount of that material is excessive, such as 50%-wt or more in lignites from India or Greece. In Germany, almost all (brown) coals are washed before firing. Waste-derived fuels and biomass fuels contain associated material that is only loosely bound to the combustible part of the fuel. Significant amounts of KCl (potassium chloride) can be removed from straw, for example, by simply washing with water. Pieces of metals such as iron and aluminum are easily removed from waste-derived fuels by magnetic and eddy current-based methods.
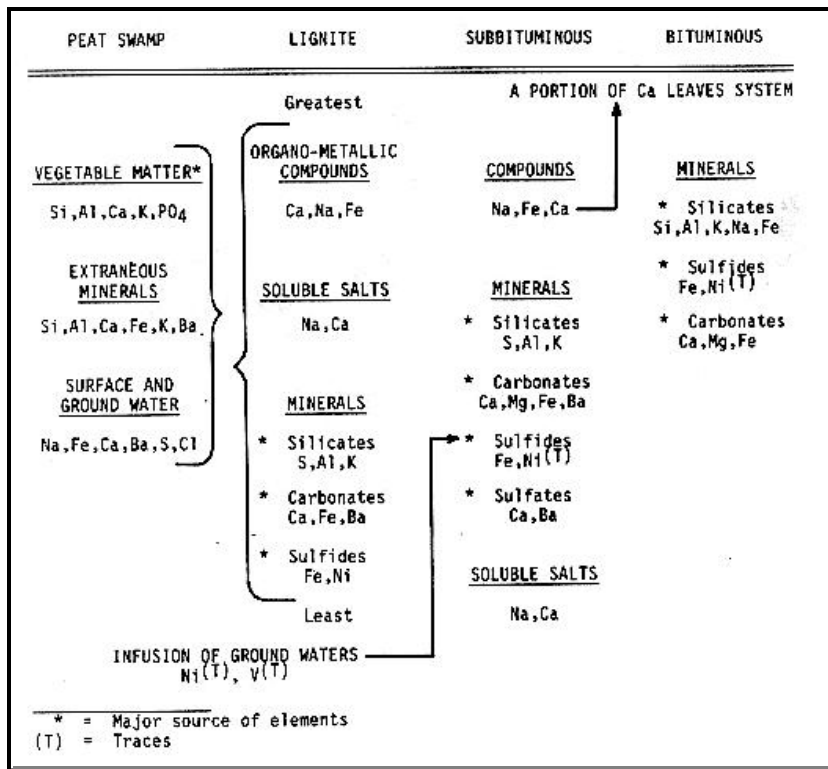
Figure 5.3 Transformation of mineral matter during coalification (picture from Bryers, 1996).

Figure 5.3 gives a schematic summary on how minerals slowly but surely become part of the coal during the coalification process. Silicates, sulphides (pyrite) and carbonates are the result of interactions between deteriorating organic material, extraneous minerals and surface and ground water.

Nonetheless, the ash-forming matter is present in the fuel in two forms: as discrete particles and as inclusions of the combustible matrix. The implications this has for the combustion or gasification process is illustrated by Figure 5.4. Discrete mineral particles are quickly isolated, and melting at high temperatures is followed by condensation during cooling after leaving the furnace. Included minerals, however,

Figure 5.4 Interactions between mineral impurities during coal combustion (picture from Sloss *et al.*, 1996).

become more and more concentrated in the fuel matrix as the connecting hydrocarbon is consumed. Metal oxides may also be reduced by the carbon, and can be released as elemental metal vapour.
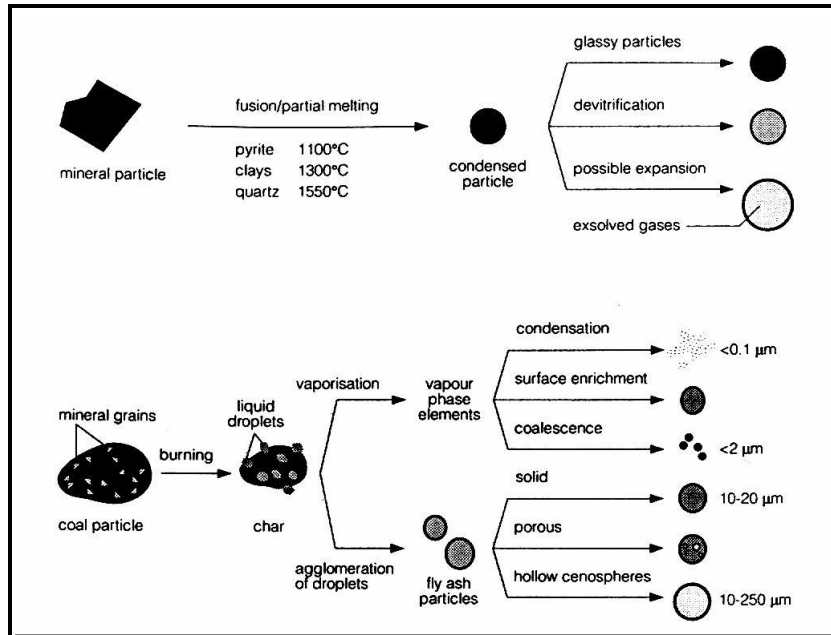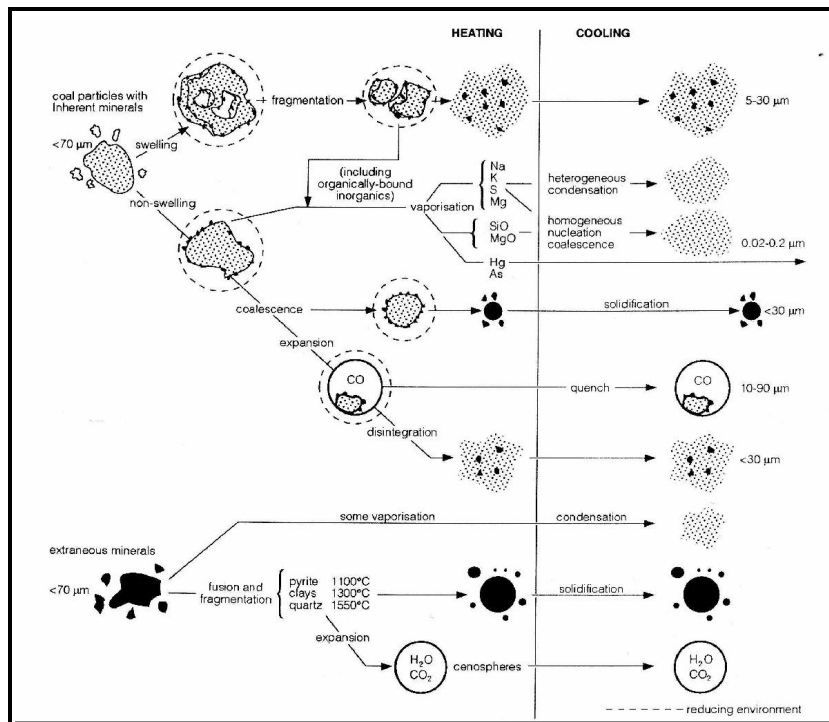
Figure 5.5   Ash formation in a pulverised coal combustor
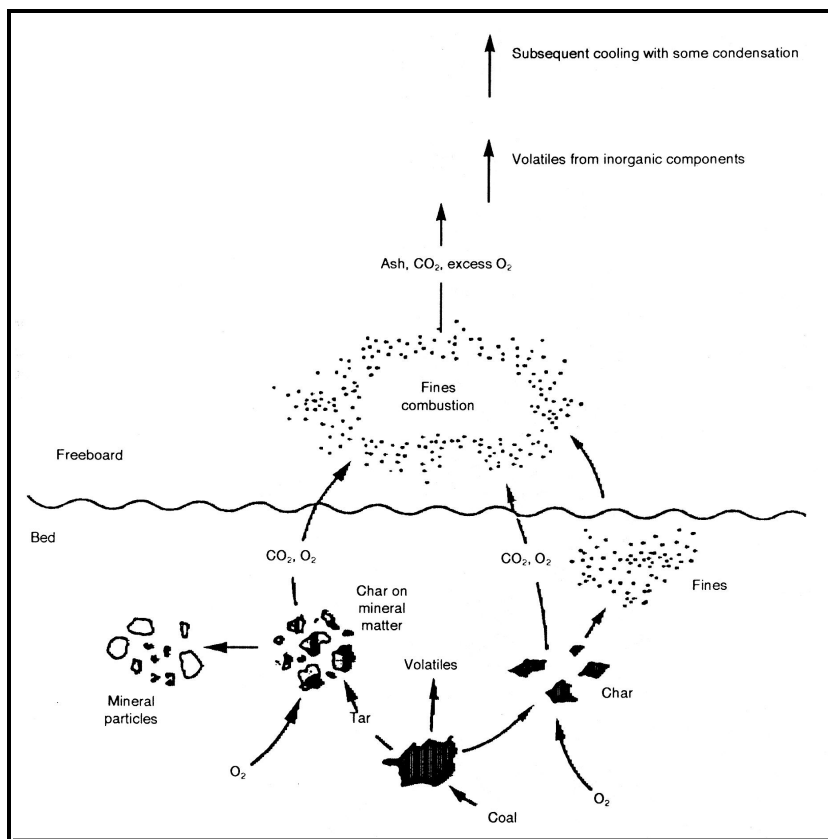(picture from Couch, 1995)

Figure 5.6   Ash formation during bubbling fluidised bed
combustion (picture from Couch, 1995)

In the gas phase these can be oxidised again, followed by some clustering and coalescence, forming a significant part of what may be eventually emitted as $PM_{2.5}$. Non-combustibles that are not vaporised will form the major part of the fly ash particles to be collected by the dust control system. Figure 5.5 shows with somewhat more detail the influences of temperature and changing particle size on the formation of ash particles ranging from 0.01 ∶ m to more than 100 ∶ m.

During gasification a different picture is seen that can be explained when considering the reducing gas atmosphere. The reduction of metal oxides to elemental metal (with a much lower boiling point) is much stronger, and re-oxidation and clustering of the oxide particles does not occur.

Something similar is seen when the chlorine content of the fuel is high (*i.e.* > 0.1 %-wt dry). In that case the metal oxides are transformed to chlorides with a much lower boiling point, followed by vaporisation. At lower temperatures these chlorides may react with water to metal oxides and HCl.

During fluidised bed combustion the fate of ash-forming material is very much different from what happens during pulverised fuel firing. Temperatures are much lower and particles are larger, but mechanical stresses are stronger due to strong turbulence and many impacts between particles. Fines are produced due to attrition and abrasion but much ash-forming material remains in the bed. This is illustrated in Figure 5.6. For a circulating fluidised somewhat more fly ash is formed due to the higher velocities and smaller fuel particle size.
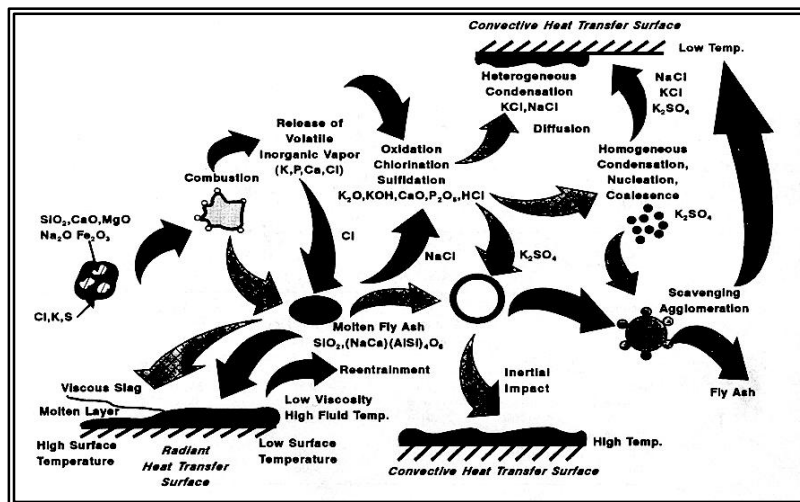

Figure 5.7   Behaviour of ash-forming matter in biomass fuels (picture from Bryers, 1996)

Biomass fuels typically produce ashes that contain 5-10 %-wt potassium, 20%-wt or more calcium (ash from wood, though, may contain 70 %-wt $CaO+CaCO_3$) and not much more than 10%-wt silica. The ash chemistry is in this case determined by species such as KOH, NaOH, KCl, NaCl, K_2SO_4, Na_2SO_4 and SiO_2, as illustrated by Figure 5.7. The ashes and deposits formed may have first melting points lower than 600EC, giving sticky deposits and/or defluidisation when biomass is fired in a fluidised bed. Also with these fuels the volatility of the ash-forming elements is higher with gasification than during combustion.

For the inorganic particles that are produced by coal combustion Sarofim and Helble (1993) give a rough procedure for calculating ash particle size. The largest fraction lies in the size range 1 - 30 μm, and is formed by coalescence of included minerals as described above. Assuming that one ash particle is formed per fuel particle, given that the average fuel particle size is d_f (m), the ash content is f_a (kg/kg dry fuel) and the densities of the fuel and ash particles are ρ_f and ρ_a (kg/m³), respectively, average fly ash particle size is approximately $d_a \sim (f_a\rho_f/\rho_a)^{1/3}d_f$. (For d_f = 50 μm, ρ_f/ρ_a = 0.5 and

f_a = 0.1 kg/kg, it is found that $d_a \sim 18.4$ μm). In addition submicron fume is formed due to vaporisation and condensation of mineral constituents, typically up to 6% of the total ash stream that leaves the furnace with the flue gas (Sarofim and Helble, 1993).

It is clear that a concept such as the "ash content" of a fuel is not easily related to the formation of bottom ashes and fly ashes during combustion or gasification as a pulverised fuel, or in a fluidised bed. Nevertheless, standard tests do exist, such as DIN and ASTM procedures (DIN, 1978), where a fuel is heated up in air under certain specific conditions. For biomass fuels, maximum test temperatures are typically a few hundred degrees lower than for coal in order to avoid loss of alkali by vaporisation. Typical values for ash contents obtained by these procedures are given in Table 5.1.

Table 5.1   Typical values for the ash content of fuels (dry %-wt)

Fossil fuels		Biomasses & waste derived fuels	
Coal, lignite	5 - 40	Wood	0.1 - 0.5
		Bark	2 - 8
Oil	< 0.1	Straw	4 - 8
Natural gas	-		
Light fuel oil	< 0.01	Sewage sludge	15 - 20
Heavy fuel oil	~ 0.04	Car tyre scrap	5 - 8
		Munical solid waste (MSW)	5 - 25
		Refuse derived fuel (RDF)	10 - 25
Peat	4 - 10	Packaging derived fuel (PDF)	5 - 15
		Auto shredder residue (ASR)	~ 25
Petroleum coke, "petcoke"	~1	Leather waste	~ 5
Estonian oil shale	~ 40		
Orimulsion™	~ 1.5	Black liquor solids	30 - 40

The composition of these ashes varies strongly between the fuels, although SiO_2, Al_2O_3, Fe_2O_3 and CaO are usually the primary components. Ash from fuel oils contains vanadium (V) and nickel (Ni), plus magnesium (Mg) which is added to the fuel as a corrosion inhibitor. Biomass ashes contain typically 5-10 % potassium (K) (Bryers, 1996). Ash from petcoke contains significant amounts of iron, vanadium and nickel (Anthony, 1995). Special ashes such as ash from leather waste combustion may contain close to 90 %-wt Cr_2O_3 (Cabanillas *et al.*, 1999).

The content of ash-forming matter in a solid fuel may easily be of the order of 10-20 %-wt (dry). The amounts of material that have to be handled for a typical power plant will therefore be significant and require a transport system by road, rail or water. This is illustrated by some numbers from a US power plant in Table 5.2.

Table 5.2   Production of ashes from western US coal combustion in a 500 MW_{elec} pulverised coal power plant (taken from Carpenter, 1998)

	Bituminous	Wyoming Powder River Basin	Montana Powder River Basin
Coal ash content, %-wt	9.5	4.8	3.7
Bottom ash, ton/year	24560	17280	8600
Fly ash, ton/year	98260	69100	34390
Total ash, ton/year	122820	86380	42990

5.3   Particulate emission standards

For coal (and peat) combustion, SO_2 emission standards for Finland (1997) and the European Community (1988) are given in Tables 5.3 and 5.4.

Table 5.3   Particulate emission standards for Finland (1997)

Type of plant	New / Existing	Plant size (MW_{th})	Emission standard $(mg/m^3_{STP}$ dry 6% $O_2)$	Comments
Combustion plant lignite, peat, wood, straw	New	1-5	540	Guideline
Combustion plant lignite, peat, wood, straw	New	5-50	(248-11*P)/3	Guideline, P=plant size in MWth
Utility, hard coal	New	1-5	405	Guideline
Utility, hard coal	New	5-50	172-2.1*P	Guideline, P=plant size in MWth
Utility, hard coal	New	50-300	50	Guideline
Utility, hard coal	New	> 300	30	Guideline
Utility, hard coal	Existing	all	see comments	Guideline for new plant used as target for existing plants

Table 5.4   *Particulate emission standards for the European Community (1988)*

Type of plant	New / Existing	Plant size (MW$_{th}$)	Emission standard (mg/m³$_{STP}$ dry 6% O$_2$)	Comments
Combustion, coal	New *	50-500	100	
Combustion, coal	New *	> 500	50	

* construction licence after July 1 1988

The World Bank suggests a worldwide emission limit for all new coal-fired units of 50 mg/m³$_{STP}$ (dry) @ 6 % O$_2$, or, if that is impossible, 99.9% removal efficiency (Soud and Mitchell, 1997, McConville, 1997).

For waste firing, the particulate emission standard for Finland (as of 1.8.1994) is 10 mg/m³$_{STP}$ (dry) @ 10 % O$_2$ (Finland, 1994). This value is also the current daily-mean emission standard for the EU15 countries. For cement plants the Finnish emission standard as of 1.1.2001 is 50 mg/m³$_{STP}$ (dry) @ 10 % O$_2$, the European Commission has proposed a future standard of 30 mg/m³$_{STP}$ (dry) @ 10 % O$_2$.

5.4   Options for particulate emissions control

Selecting the most suitable device for the removal of particles from a gas stream depends on many things, partly determined by the process *i.e.* gas stream, partly determined by the particles that are to be removed. A summary of the most important factors that are to be considered is given in Table 5.5. When high temperature, high pressure (HTHP) gas clean-up is required (∟ section 5.11) the range of possible options is more narrow than when an atmospheric process is needed that operates below 200EC. Another important factor is size: filters are available from very small sizes (consider a sigarette filter) to large baghouse units with hundreds of separate filter bags. Electrostatic precipitators (ESPs), on the other hand, cannot be operated economically in flue gases of power units smaller than a few MW$_{thermal}$.

Size and size distribution are the most important particle-related factors, followed by their physical and chemical properties: the particles should not destroy the control device, but they should not be "invisible" to the control device either. Low sulphur coal, for example, can produce ashes that do not allow for sufficient electrostatic charging, making these particles hard to handle by an ESP.

Table 5.5   Process- and particle-dependent factors for selecting a particulate control device

Process-dependent factors	Particle-dependent factors
Gas flow volume	Particle size and size distribution
Temperature	Shape of the particles
Pressure	Surface properties
Composition of the gas	Chemical stability
Concentration of particles in the gas	Mechanical strength *etc.*, physical properties
	Chemical composition: carbon, alkali, tar, sulphur content
	(First) melting point, softening point

All this has to be related to the final objective, which is reducing the particle concentration to a certain level, with additional specifications for the outlet particle size distribution. For coal combustion by different methods the typical uncontrolled emissions and the required control efficiencies for obtaining a certain maximum outlet concentration are given in Table 5.6. Cyclone firing gives relatively low fly ash emissions, with a relative small size, though, while stoker (*i.e.* grate) firing gives somewhat higher emissions, at a relatively wide particle size distribution. The highest emissions are generated by pulverised coal units. Altogether, for a typical emission standard of 50 mg/m³$_{STP}$ the efficiency of the control system has to be of the order 95 - 99%.

Table 5.6   Particulate control efficiencies required for a certain controlled emission (in %) for various coal-fired boilers (taken from Klingspor and Vernon, 1988)

Boiler configuration	Uncontrolled emissions g/m³	Controlled emission limits 50 mg/m³	100 mg/m³	200 mg/m³	500 mg/m³
Pulverised coal	8–20	99.37–99.75	98.75–99.50	97.50–99.00	93.75–97.50
Spreader stoker	2–5	99.00–99.50	95.00–98.00	90.00–96.00	75.00–90.00
Chain grate stoker	1–3	95.00–98.30	90.00–96.70	80.00–93.33	50.00–83.33
Cyclone	0.5–1.5	90.00–96.67	80.00–93.33	60.00–87.67	0.00–66.67

Finally, it is noted that different devices operate in different particle size ranges. This is a result of the physics that lies behind the method by which the particles are manipulated and eventually removed from the gas stream. As illustrated by Figure 5.8, these can be separated in processes where an external force is applied to the particle

and processes where the gas stream is forced through a barrier that cannot be passed by the dispersed particles, in the form of holes smaller than the particles, or a droplet cloud.
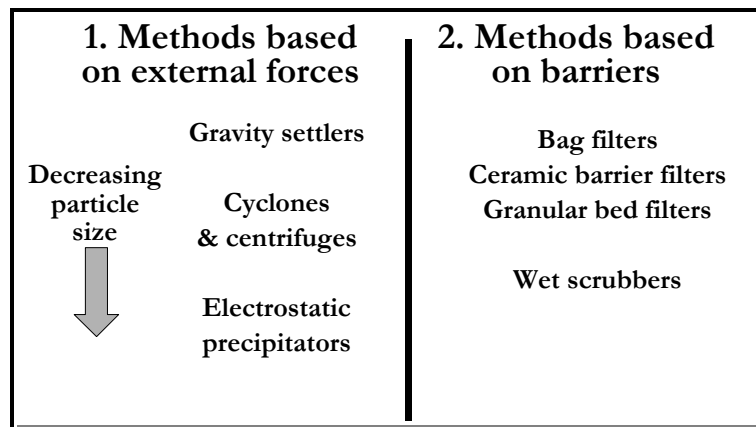
1. Methods based on external forces	2. Methods based on barriers
Gravity settlers	Bag filters
Decreasing particle size →	Ceramic barrier filters
Cyclones & centrifuges	Granular bed filters
	Wet scrubbers
Electrostatic precipitators	

Figure 5.8   General classification of particulate control devices

For a few types of particulate control device the removal efficiencies are given for four particle size ranges in Table 5.7. For larger particles (> 10 µm) gravity and centrifugal forces can be effective, for fine particles (< 2 µm) an electrostatic force can be applied, in combination with particle charging. Venturi scrubbers operate down to a few micrometer, whilst filters offer very high efficiencies over wide size ranges. This comparison already shows the large potential of filter systems: they give high removal efficiencies over wide size ranges and they are more flexible than other method when considering the properties of the

Table 5.7   Collection efficiencies (in %) of several particulate control devices (table from Soud, 1995)

Control device	Removal efficiency			
	<1 µm	1–3 µm	3–10 µm	>10 µm
High efficiency ESP	96.5	98.25	99.1	99.5
Fabric filter	100	99.75	>99.95	>99.95
Venturi scrubber	>70	99.5	>99.8	>99.8
Multicyclones	11	54	85	95

particles and the process conditions. A drawback is that relatively low gas velocities must be used, which directly translates to large filtration surface and inherently high costs.

In the remainder of this chapter the various methods are discussed, based on Figure 5.8. High temperature/high pressure methods (HTHP) receive special attention.

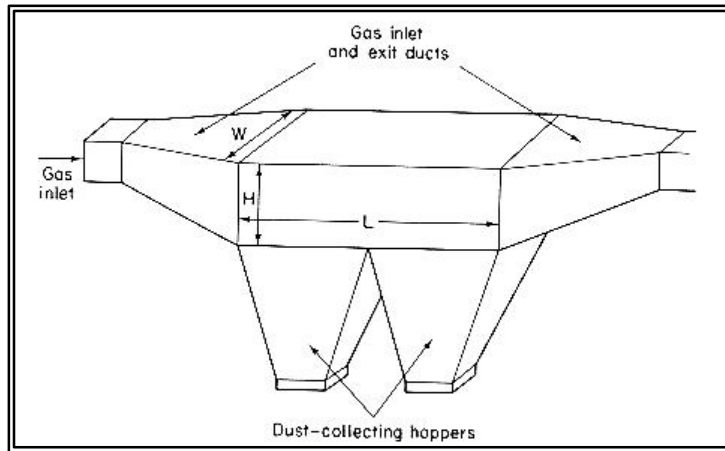## 5.5   Gravity settlers

Figure 5.9   Typical lay-out of a gravity settler (picture from Flagan and Seinfeld, 1988)

Large particles, with sizes ranging from 50 μm to more than 1 mm may be successfully removed by a gravity settler, as shown in Figure 5.9. As a result of a sudden widening of the flue gas channel the gas velocity is reduced, which increases the response of the particles in the gas stream to gravity. This will induce a downwards motion towards dust collecting hoppers that constitute the floor of the device. A drawback of these devices is their huge size and the problems related to the erosion wear experienced by the dust-collecting hoppers.

Depending on the gas velocity, laminar flow or turbulent flow settling chambers can be distinguished, for flow Reynolds numbers smaller or larger than ~ 4000, respectively. For a settler as shown in Figure 5.9, processing a gas stream with velocity u (m/s), density $\mathbf{r}_{gas}$ (kg/m³) and dynamic viscosity $\mathbf{h}_{gas}$ (Pa.s), the Reynolds number of the flow, using the hydraulic diameter d_H, is defined by:

$$Re = \frac{2\,d_H\,u\,\mathbf{r}_{gas}}{\mathbf{h}_{gas}} = 2\,\frac{H\,W}{H+W}\,\frac{\mathbf{r}_{gas}}{\mathbf{h}_{gas}} \tag{5-2}$$

Turbulent setlling chambers have somewhat lower collection efficiencies than laminar settler since the intense turbulent mixing prevents the settling. The efficiencies for laminar and turbulent settling chambers, the two extreme cases, are given by (Flagan and Seinfeld, 1988):

$$Laminar:\;\; Efficiency\,(d_p) = \frac{u_t\,L}{u\,H} \tag{5-3}$$

$$Turbulent:\;\; Efficiency\,(d_p) = 1 - exp\left(-\frac{u_t\,L}{u\,H}\right)$$

where u_t is the terminal settling velocity of the particles (☞ Appendix to this chapter).
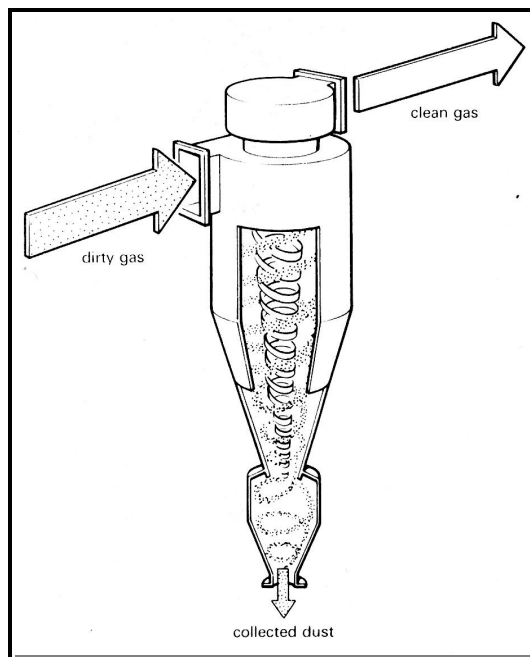
5.6   Cyclones

Figure 5.10   A typical gas cyclone (picture from Klingspor and Vernon, 1988)

5.6.1 Principle of operation, lay-out

A cyclone is a mechanical separator that is capable of reducing dust concentrations in a gas stream from several g/m³ to below 0.1 g/m³. The principle of operation is to force the flow into a swirling motion with high tangential velocities, inducing tangential forces on the particles that are of the order of several hundred times gravity. An impression of a gas cyclone and the flow field inside a cyclone is given in Figure 5.10, showing an outer, downwards vortex surrounding an inner, upwards vortex. The pressure distribution inside a cyclone is such that at the bottom outlet for the collected particles the gas stream is forced to turn upwards. Particles that are flung to the wall by the centrifugal forces will flow downwards along the wall towards the bottom outlet: some part may be re-entrained into the gas stream, though. Cyclones are applied also for removing *e.g.* water from oil at oil fields ("hydrocyclones").

Cyclones are considered to be very powerful and cheap pre-separators for gas clean-up purposes. Their removal efficiency is, however, limited to ~ 90% for a cyclone of reasonable size (diameters up to 1 m) with reasonable pressure drop, and the removal efficiency rapidly deteriorates for particles smaller than 10 μm. The most important pro's and contra's of the use of gas cyclones is given in Table 5.8.

Table 5.8   Characteristics of gas cyclones

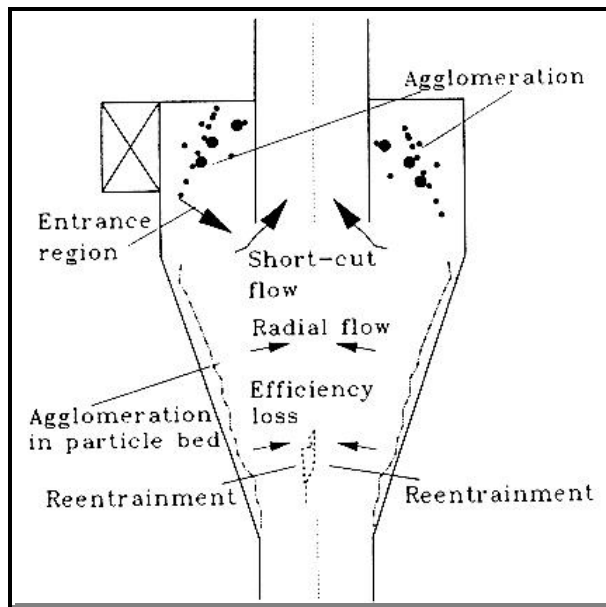| Advantages	Disadvantages
Simple	Large pressure drop
Cheap	Low efficiency
Compact	"Catch" removal problems
Large capacity	No particle removal below ~ 5 μm
	Problems at temperatures above ~ 400EC

Figure 5.11   Processes determining gas cyclone separation efficiency (picture from Bernard, 1992)

Cyclones are being used at temperatures up to and above 1000EC, for example in PFBC systems (**7** chapter 2). By applying two or three units in series acceptable removal efficiencies may be obtained.

The removal efficiency of a cyclone is affected by many "side-processes" due to the design of the cyclone, the flow pattern and the pressure profile. The most important are shown in Figure 5.11. Agglomeration of particles at the inlet region is the result of stronger centrifugal forces on larger particles than on smaller ones, causing a "sweeping" effect. At the same time, particles may short-cut from the inlet to into the gas outlet when the outlet tube, called "vortex finder" does not penetrate deep enough into the cyclone from above. Going downwards along the wall, the layer of collected particles may come in contact with the flow field of the gas flow, leading to re-entrainment. Most critical is the position near the bottom outlet for the collected dust, where the downwards swirl turns upwards into the inner vortex towards the gas outlet. At that point strong re-entrainment of collected particles may occur, which most certainly will leave the cyclone with the gas (Bernard, 1992).

Depending on the application, three types of gas cyclones can be distinguished: besides a "conventional" cyclone one may select either a "high efficiency" or a "high throughput" design. The latter compromises efficiency at the benefit of higher throughput and lower pressure drop, the opposite can be chosen as well. For the widely used, so-called "Lapple" cyclones, design parameters are given in Figure 5.12 and Table 5.9 (Cooper and Alley, 1994). Typical gas inlet velocities are 15 - 30 m/s.
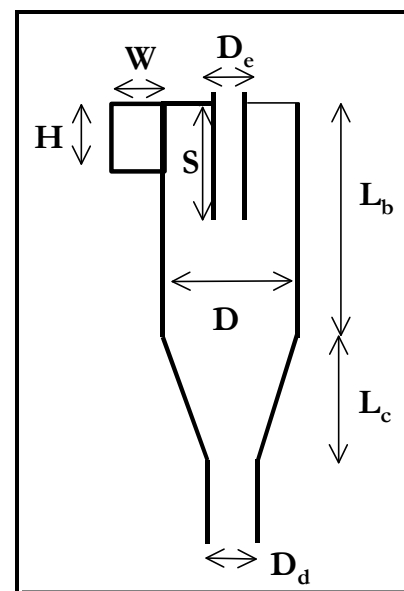

Figure 5.12   Lapple cyclone design lengths (after Cooper and Alley, 1994)

Table 5.9   Design parameters for a Lapple cyclone (see Figure 5.12)

	High efficiency	Conventional	High throughput
Height of inlet H/D	0.5 ~0.44	0.5	0.75 ~ 0.8
Width of inlet W/D	0.2 ~ 0.21	0.25	0.375 ~ 0.35
Diameter of gas exit De/D	0.4 ~0.5	0.5	0.75
Length of vortex finder S/D	0.5	0.625 ~ 0.6	0.875 ~0.85
Length of body Lb/D	1.5 ~1.4	2.0 ~1.75	1.5 ~1.7
Length of cone Lc/D	2.5	2	2.5 ~2.0
Diameter of dust outlet Dd/D	0.375 ~ 0.4	0.25 ~ 0.4	0.375 ~ 0.4

5.6.2 Removal efficiency, pressure drop

The efficiency of a cyclone can be described (as for any particulate control device discussed in this chapter) by a so-called "grade efficiency curve", which gives the removal efficiency as function of particle size. An important number is the so-called "cut-size", d_{50}, which is the particle size for which the removal efficiency is 50%. For particles larger than the cut size more than 50% is removed, for particles smaller than the cut size removal efficiency is less than 50%. For cyclones such as the Lapple cyclones the "cut size" can be calculated as:

$$d_{50} = \sqrt{\frac{9\,\eta_{gas}\,W}{2\,\pi\,V_i\,(\,\rho_{solid} - \rho_{gas})}} \quad with \quad N = \frac{L_b + \frac{1}{2}\,L_c}{H} \qquad (5-4)$$

where W is the width of the gas inlet (m), V_i the inlet gas velocity (m/s), ρ_{solid} and ρ_{gas} the densities of solid particles and gas, respectively, (kg/m³), η_{gas} is the dynamic viscosity of the gas (Pa.s) and N is the number of rotations (#) the gas flow makes before turning upwards to the vortex finder. For a Lapple cyclone, N is apparently defined given by the dimensions of the cyclone (see Figure 5.12).

The "grade efficiency" of the cyclone can be described as a relation between particle size, d_p , and cut size d_{50}:

$$Eff\,(\,d_p\,) = \frac{1}{1 + (\frac{d_{50}}{d_p})^2} \qquad (5-5)$$
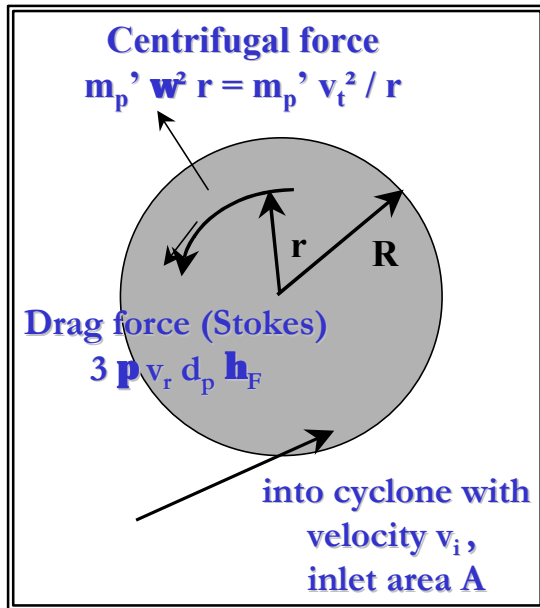
Figure 5.13 Particles in cyclones (top view): forces on a particle (Zevenhoven and Heiskanen, 2000)

The calculation of cut size by eq. (5-4) follows from considering the force balance on a particle in a cyclone as shown in Figure 5.13. For a particle with volume V_p the reduced mass m'_p equals $V_p(\rho_{solid} - \rho_{gas})$, with particle and gas densities ρ_{solid} and ρ_{gas}. A force balance, *i.e.* equating the centrifugal force to the drag force gives

$$\frac{m'_p v_t^2}{r} = 3 p v_r d_p h_F \qquad (5\text{-}6)$$

for a particle at radial position r, using Stokes' Law for the drag force (☞ Appendix). The radial and tangential velocities v_r and v_t can can be approximated by

$$v_r \approx \frac{V_i A}{2 p r h} \; where \; h = length \; scale \; for \; the \; cyclone$$

$$(5\text{-}7)$$

$$v_t \, r^n = V_i \, R^n \qquad where \; n = 0.5..0.55 \; for \; a \; gas \; cyclone$$

An estimation for the cut size is then found assuming that a particle with size $d_p = d_{50}$ will move at force equilibrium at radial position r=R:

$$\left(\frac{r}{R}\right)^n = \frac{p \, h \, r_{solid} \, V_i \, d_p^2}{9 \, A \, h_F} \; which \; gives$$

$$(5\text{-}8)$$

$$with \; d_p = d_{50}, \; r = R \; the \; result \; is \; d_{50} = \sqrt{\frac{9 \, A \, h_F}{p \, h \, r_{solid} \, V_i}}$$

which is identical to eq. (5-4) when A=H×W and h=2L$_b$+L$_c$.

Pressure drop is the second important cyclone performance characteristic, after collection efficiency. It can be estimated by:

$$\Delta p = \frac{1}{2} \frac{r_{gas} V_i^2 \, K \, H \, W}{D_e^2} \quad (Pa)$$

(5-9)

which contains the design dimensions H, W and D_e (see Figure 5.12). For the constant K, the value 12 ~ 18 is suggested, with K=16 as recommended value (Cooper and Alley, 1994).
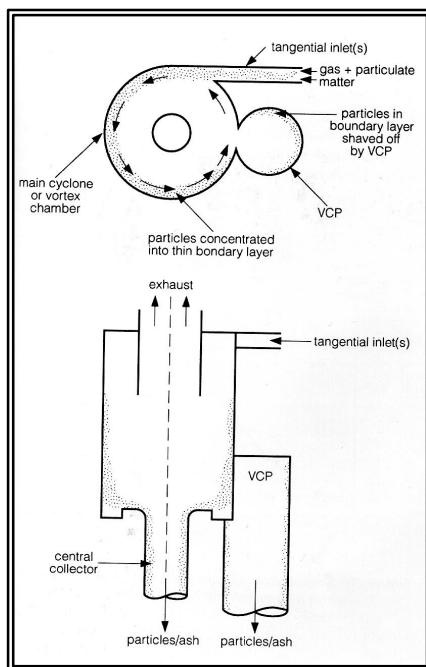
5.6.3 Developments in gas cyclone design

Figure 5.14   Gas cyclone with collector pockets (picture from Soud, 1995)

Two design concepts for improved gas cyclones are shown in Figures 5.14 and 5.15 (Soud, 1995).

In the first design, one or more vortex collector pockets (VCPs) are attached to the main cyclone with the objective to improve the removal efficiency of the finest particles. Advances might be reduced height and pressure drop.

The other design, the so-called aerodyne rotary flow cyclone operates with two vortices in opposite direction: the first being the flue gas that is entered through a stationary spinner, the second vortex enters from the top. The result is a net downwards flow for the particulates whilst the main gas steam moves upwards. The (clean) secondary gas flow should be of the order of ⅔ of the primary gas stream: using the dusty gas to be cleaned also as the secondary gas stream gives a much worse removal performance.

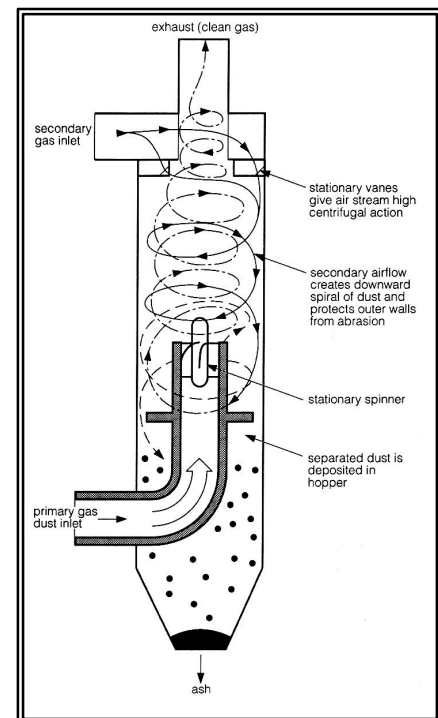**Figure 5.15**   Aerodyne rotary flow cyclone (picture from Soud, 1995)

5.7   Electrostatic precipitators (ESPs)

5.7.1 Principle of operation, lay-out

The removal of particles using electrostatic precipitator, hereafter abbreviated ESP, is based on applying a surface force instead of a body force to fine particles. The surface of the particles is where the electrostatic charge is residing. Combined effects of the particle production or formation process and further processing such as transport along a conveying system or flue gas duct result in sometimes large electrostatic charges on solid particulates or droplets. For gas clean-up this charge is generally too low, however. The combination of particle charging, extracting the particle or droplet from the gas stream and deposition on a collection plate system is the general procedure that is referred to as electrostatic precipitation.

For fly ash emission control from combustion and gasification of fossil fuels, mainly coal and peat, ESPs are the most widely used technology. Outside what can be called the "developed world" (EU, North America, Japan and Australia) an ESP for fly ash emission control is generally the only emission control system used at electric power stations. Reasons for this are obvious: the technique of ESP is rather simple, it offers high removal efficiencies at low pressure drop and low electric power consumption, and the electricity needed to operate the system is readily available.

Typical power consumption of an ESP is of the order of 0.05 - 0.3 W per m_{STP}^3/s gas volume (Cooper and Alley, 1994). Comparing this to a flue gas production rate for a typical coal-fired power plant, which is 0.3 - 0.4 m^3_{STP}/MJ$_{thermal}$ shows that the "internal" electric power consumption of an ESP unit is very small.

The typical features of an ESP are shown in Figure 5.16 for a wire-
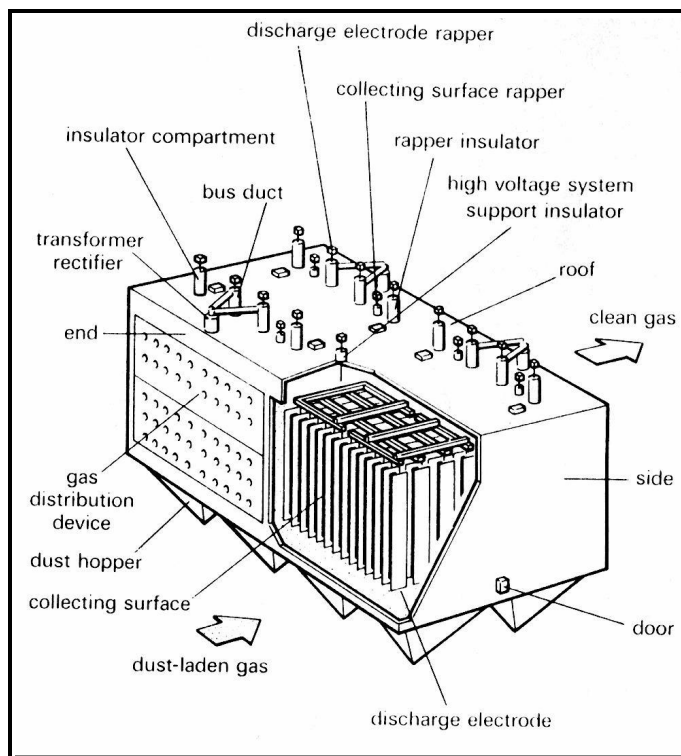

Figure 5.16   Typical lay-out of an ESP (picture from Klingspor and Vernon, 1988)
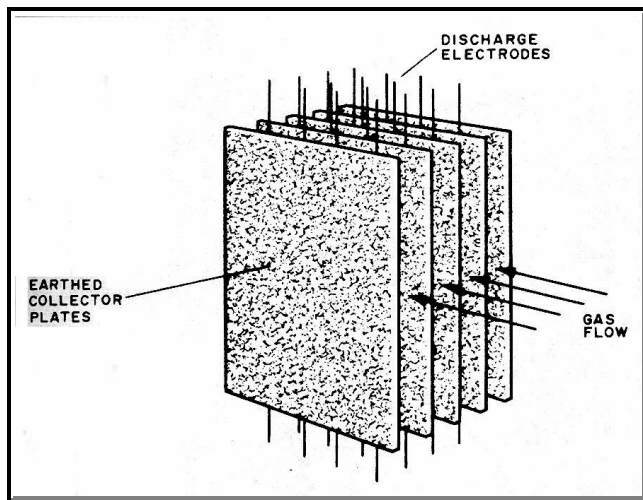
Figure 5.17   Schematic electrode geometry for a wire-and-plate ESP (picture from Coulson and Richardson, 1978)

1 — discharge electrode; 2 — tensioning weight; 3 — suspension frame; 4 — suspension rod; 5 — insulator; 6 — suspension-rod sheath; 7 — guide (spacer) frame; 8 — collecting electrode; 9 — casing; 10 — inlet stub; 11 — outlet stub; 12 — hopper; 13 — inlet plenum chamber; 14 — outlet plenum chamber; 15 — dust discharge port.

Figure 5.18   Typical layout of a wire-in-tube ESP (pictures from Böhm, 1982)

and-plate unit operated with a horizontal gas flow. A schematic picture of the electrode geometry for this is shown in Figure 5.17. A wire-in-tube ESP design is shown in Figure 5.18 - note that the gas flow is upwards !

Four process steps are involved in particle (or droplet) removal by ESP:

1.   Charging of the particle
2.   Particle movement relative to the gas flow
3.   Particle deposition on a collection surface
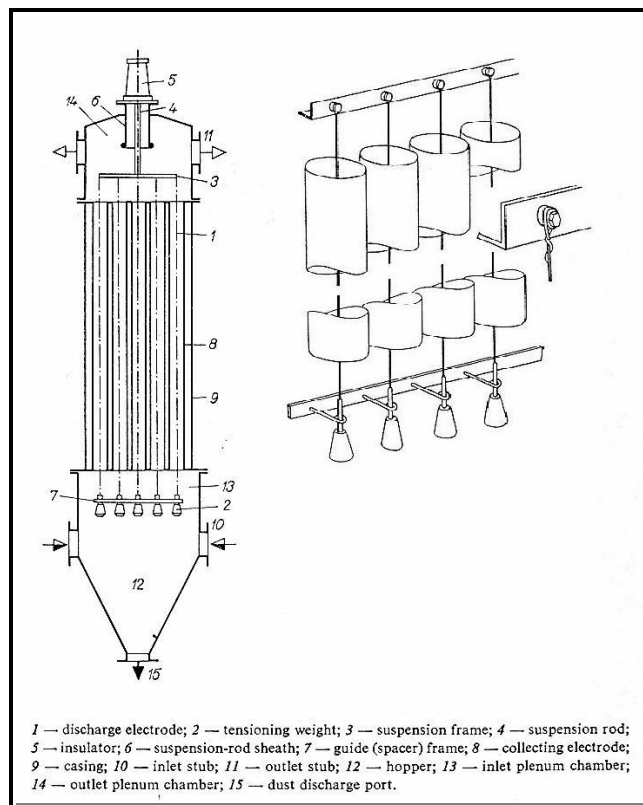4.   Removal of the deposited particles from the system

This is further illustrated by Figure 5.19 for a system where a corona discharge is used to put an electrostatic charge (unit: Coulomb, C) on the particles. This charge will be much higher than the charge they already possess, and comes close to the maximum charge the particle can carry.

5.7.2 Corona discharge

Corona particle charging employs ions that are generated at the discharge electrodes which, together with the collector plates produce a highly non-uniform electric field. In general this is accomplished by putting direct current (DC) high voltages of the order of 30 to 75 kV on the discharge electrodes and earthing the collector plates. If the electric field intensity, E, (unit: V/m) becomes larger than the electric breakdown intensity (which
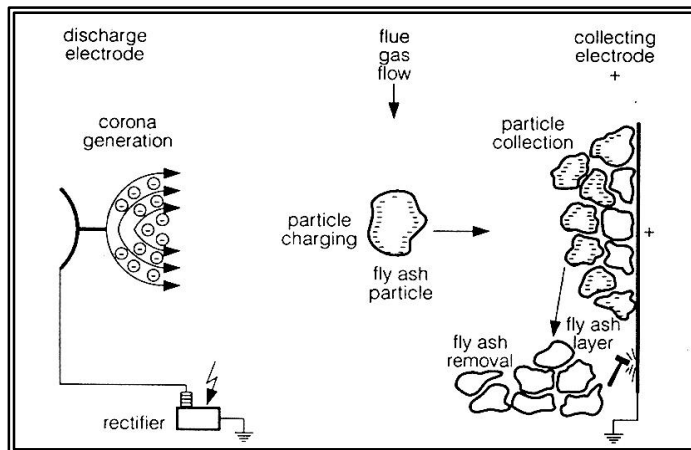
Figure 5.19   Particle charging and collection in ESP (picture from Soud, 1995)

is ~30 kV/cm for ambient air), ions such as N_2^+ and O_2^+ and electrons, e^-, are produced at the electrode. When operating at negative potential the electrons will travel towards the other electrode, whilst the positive ions will move to and collide with the electrode and become neutralised. Under positive corona operation the positive ions will move across the space between the electrodes after the discharge electrode has taken up the electrons. More detail on electric breakdown and corona discharge processes is given elsewhere (Böhm, 1982, Kuffel and Zaengl, 1984).

5.7.3 The electric field

The electric field strength (or intensity) E is defined by the electrode geometry and the voltage difference $\Delta\phi$ (unit: Volt, V) that is applied between them:

$$\underline{E} = -\nabla f \quad with \ \nabla = (\partial/\partial x, \partial/\partial y, \partial/\partial z)\ (in\ Cartesian\ coordinates) \qquad (5\text{-}10)$$

In ESPs the electric field is basically 2-dimensional, without significant electric fields in the gas flow direction. For practical reasons, the electric field strength is related to the distance, x (m) from the centre of the discharge electrode and a "configuration factor for the electrode geometry", F (-), resulting in a one-dimensional description of the electric field:

$$E(x) = \frac{\Delta f}{F\,x} \qquad (5\text{-}11)$$

For a wire and plate geometry as shown in Figures 5.16 an 5.17, the values for F are calculated as shown in Figure 5.20 for one wire between plates (b), for multiple wires between plates (c) and for a
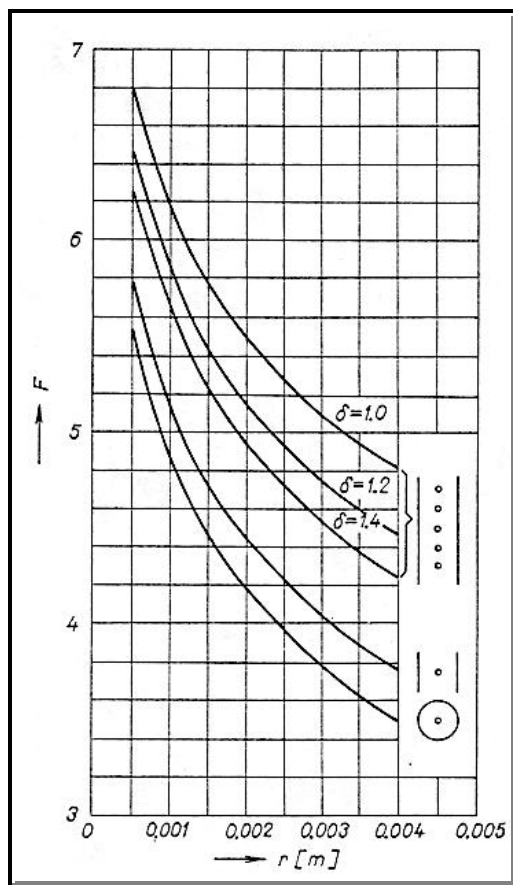

Figure 5.20   Electrode system configuration factors, F. $\delta = d/r$, d = distance between wires, r = wire radius (picture from Böhm, 1982)

Figure 5.21   Electrode system configuration factors - see also Figure 5.20 (picture from Böhm, 1982)

wire-in-tube geometry as shown in Figures 5.18 (a). For a wire-in-tube ESP the electric field strength and the equipotential lines are shown in Figure 5.22. Electrode geometry factors, F, are collected in Figure 5.21 for different geometries and discharge wire electrode radius, r (m) combinations.
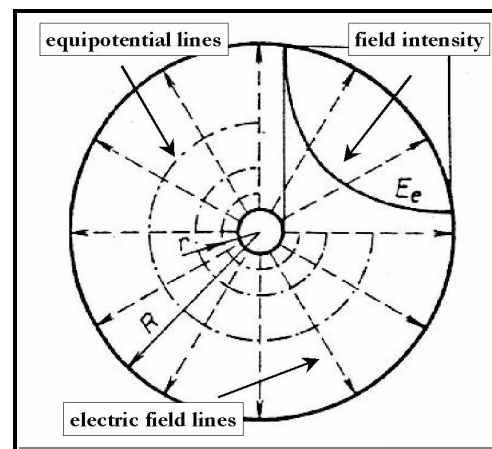

Figure 5.22   Electric field for a wire in tube ESP (after picture from Böhm, 1982)

The electric field created by the electrode system is affected by the presence of the electrons, charged ions and charged particles in the gas stream. This alters the electric field strength especially near the collection electrode (see *e.g.* Böhm, 1982)

5.7.4 Particle charging

The success of ESP operation depends primarily on the charging of the particles. Two corona charging processes are distinguished, being diffusional charging and field charging respectively. Diffusional charging implies that the particle or droplet to be charged is charged by diffusion interactions with a cloud of ions. For fine particles (smaller than ~ 0.5 μm) this will be the most important charging mechanism.

The maximum charge that can be acquired by a particle by diffusion charging depends mainly on particle size d_p (m) :

$$q_{max, diffusion} \sim 10^8 \, e \, d_p \quad (C) \tag{5-12}$$

where e is the unit charge, *i.e.* the charge of an electron: e = 1.6H10^{-19} C.

Larger particles cannot be charged to a sufficiently high level by diffusion charging alone and are charged by the field charging mechanism. As a result of the electric field in the ESP the motion of the ions and electrons is ordered along the direction of the electric field. This leads to high rates of collisions between ions or electrons and the particles, resulting in high charge levels. The maximum particle charge depends on the properties of the particle, its size, d_p, and the intensity of the external electric field, E_0:

$$q_{max,\,field} = 4\,\pi\,\varepsilon_0\,E_0\,d_p^2\,\frac{3\varepsilon_r}{\varepsilon_r + 2} \quad (C) \qquad (5\text{-}13)$$

Here, ε_0 is the dielectric constant of vacuum (ε_0 = 8.854H10^{-12} C/Vm) and ε_r (-) is the relative dielectric constant of the particulate matter or droplet (relative to vacuum) that is charged. (The dielectric constant $\varepsilon = \varepsilon_0\,\varepsilon_r$ determines whether or not the field lines of the electric field can go through the particle (ε_r ~1) or are deflected around the particle (ε_r 6 4), and is related to the optical refractive index). The definition of maximum charge eq. (5-13) shows that a particle with a high ε_r can be charged to three times the level of a particle with low ε_r.

The charge that a particle or droplet eventually acquires depends on three additional factors, being time, the concentration of ions in the charging zone N_0 (#/m³) and the electric mobility of these ions, Z_i (m/s) /(V/m)), which determines the velocity of the ions, v_i (m/s) in response to the electric field E_0. Typical values for E_0 in the charging zone are 10^6 V/m. A theoretical description of the field charging process was given by Pauthenier and Moreau-Hanot (1932), see also Böhm (1982), or Zevenhoven (1999).
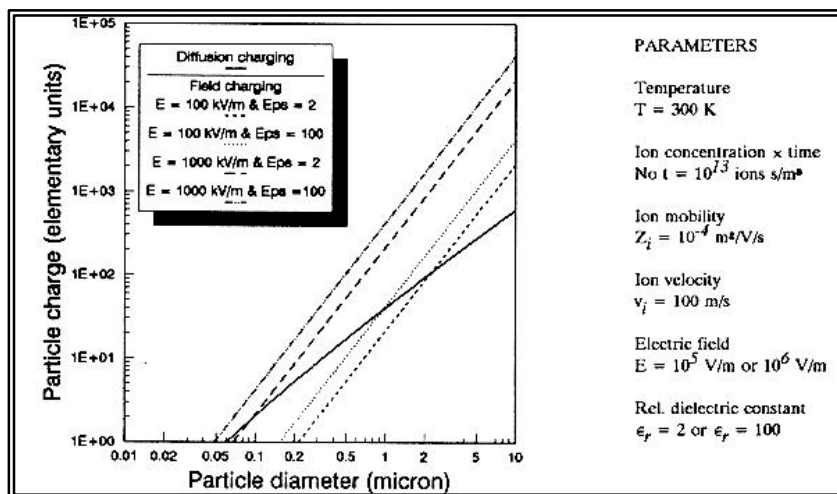
A comparison between particle charging according to the diffusion mechanism and the field charging mechanism for low and high values for ε_r and E_0 is given in Figure (5.23) for particle size 0.01 - 10 μm, at 300 K.

Figure 5.23   Field charging and diffusion charging of particles
(picture from Zevenhoven, 1992)

Figure 5.23 shows that for particles smaller than 0.2 μm diffusion charging is the most important mechanism, for particles larger than 2 μm field charging dominates.

Corona charging with ions of one polarity (+ or -) that travel in one direction may be the most important charging method, but alternative techniques are being used as well. Charging by impaction with other surfaces, refered to as contact charging or tribo-charging is also possible. Other methods use bi-polar ions (+ and -), and/or ions or electrons that travel through the charging space in alternating directions. A widely used method is the pulsed corona technique, which implies that the voltage at the charging electrode is increased to values that could cause spark-over, during a short pulse time that is too short for actual spark-over to occur though (CIEMAT, 1998, Scott, 1997).

5.7.5 Electrical drift velocity of charged particles

The result of the charging efforts is that the particle or droplet is accelerated in the direction of the electric field, *i.e.* will get a drift velocity in a direction other than that of the gas flow. Typically the electric fields are of the order 10 kV/m, which is one or two orders of magnitude lower than in the field charging zone. The electrical drift velocity, v_e, (m/s) of the particles can be evaluated by equating the electrostatic force on a particle with charge q_p to the viscous drag force, which can be estimated by Stokes' Law, if necessary with a Cunningham correction factor for very fine particles (☞ Appendix):

$$q_p\, E = 3\, \pi\, v_e\, d_p\, \eta_{gas} \tag{5-14}$$

Combining this with the maximum charge the particles can acquire by the diffusion charging and field charging mechanisms, eqs. (5-12) and (5-13) gives the following estimates for the electrical mobility:

$$fine\ particles\ , diffusion\ charging:\ v_e \sim \frac{10^8\, e\, E}{3\, \pi\, \eta_{gas}} \sim 0.01\, (\,m/s\,)$$

$$\tag{5-15}$$

$$large\ particle\ ,field\ charging:\ v_e \sim \frac{E\, E_0\, \varepsilon_0\, d_p\, \varepsilon_r}{\eta_{gas}\, (\,\varepsilon_r + 2\,)} \sim 0.1...1\,(\,m/s\,)$$

where E_0 and E are the electric field strength in the corona discharge zone and in the charging zone, respectively.

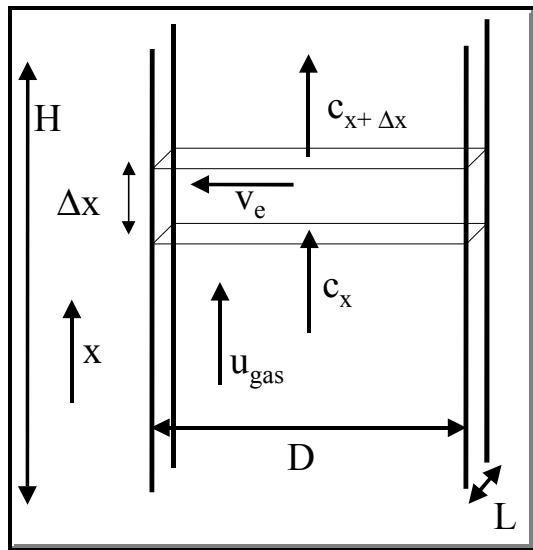### 5.7.6 Removal efficiency, Deutsch equation

Figure 5.24   ESP geometry used for efficiency analysis (Zevenhoven and Heiskanen, 2000)

The removal efficiency of an ESP is directly related to the electrical drift velocity of the particle. Based on the geometry given in Figure 5.24 an efficiency can be derived, following the approach by Deutsch from 1922 for an ESP with plate height H (m), plate distance D (m), depth L (m), gas velocity u_{gas} (m/s). The electrical drift velocity of the particle is v_e (m/s), particle concentration is referred to as c (kg/m³).

A mass balance for a small section with thickness ªx gives in-out=removed, gives:

$$\tfrac{1}{2}\, u_{gas} HLD\left(c_{at\,x} - c_{at\,x\%ª_x}\right) = v_e HL\,{}^ª x\,\tfrac{1}{2}\left(c_{at\,x} + c_{at\,x\%ª_x}\right)$$

$$Taylor\,series,\ small\ {}^ª x\,\textbf{6}\,dx:\quad \tfrac{1}{2}\,u_{gas} D\frac{dc}{dx} = v_e c \tag{5-16}$$

$$integrate\,from\ c = c_{in}\ at\ x=0:\quad c(x) = c_{in}\exp\left(\&\,\frac{2v_e x}{u_{gas} D}\right)$$

Integrating this over the height H, from gas inlet to gas outlet, noting that the flow through the section is Q (m³/s) = u_{gas}×D×L, noting that the collector surface (2 sides!) is equal to A (m²) = 2×H×L, gives the famous Deutsch equation for particle removal efficiency:

$$Efficiency\ {}'\ \frac{c_{in} - c_{out}}{c_{in}} = 1 - \exp-\left(\frac{v_e A}{Q_{gas}}\right)$$

$$with\ Matts\text{-}\ddot{O}hnfeldt\ correction: \tag{5-17}$$

$$Efficiency\ {}'\ 1 - \exp-\left(\frac{v_e A}{Q_{gas}}\right)^k\quad k = 0.4\dots0.6$$

The correction factor by Matts-Öhnfeldt was presented in the 1970s, based on
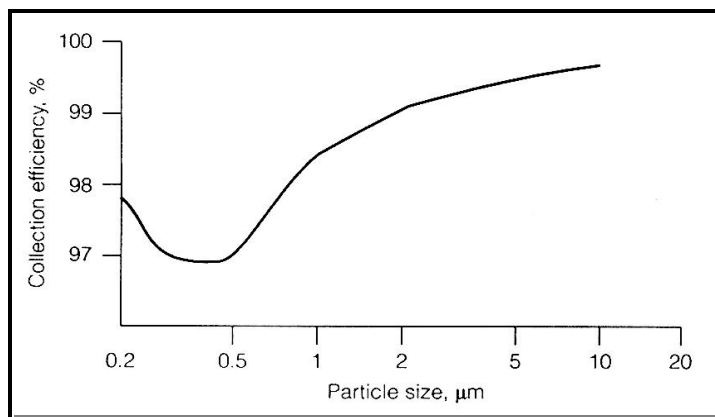
Figure 5.25   A typical grade efficiency curve for an ESP (picture from Soud, 1995)

particle size distribution and other dust-related properties, and allows for a better description of ESP performance (Klingspor and Vernon, 1988). Typically, k=0.5.

A general grade efficiency curve for an ESP is shown in Figure 5.25.

5.7.7 Effects of particle and gas properties, and temperature

It was already mentioned above that the properties of the particles or droplets to be removed, besides their size, have an effect on the particle charging behaviour and hence the removal from a gas stream by an ESP. This is made more complicated by interactions between the particle or droplet and the gas, plus the effect of temperature. Some implications this has are illustrated by Figure 5.26, which gives the effect of temperature and coal sulphur content on coal fly ash resistivity.

The temperature curves shown in Figure 5.26 (*right*) are the result of increasing surface resistivity combined with decreasing volume resistivity with increasing temperature. Depending on the chemical composition of the fly particles considered
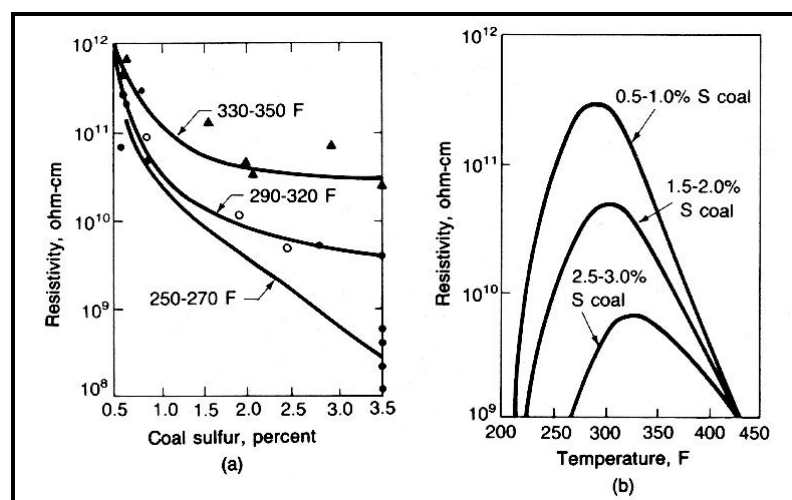

Figure 5.26   Influence of temperature and coal sulphur content on fly ash resistivity (pictures from Cooper and Alley, 1994) Note: 200EF ~ 95EC, 300EF ~ 150EC, 450EF ~ 220EC

here this gives a maximum resistivity at between 140 and 170EC. From an ESP point of view, the resistivity of the particles is preferably in the range 10^5 - 10^{10} ohm.cm. When the resistivity is very high (> 10^{11} ohm.cm) it will be difficult to charge the particles and back-corona problems may arise, *i.e.* a spark from the collection plate to the discharge
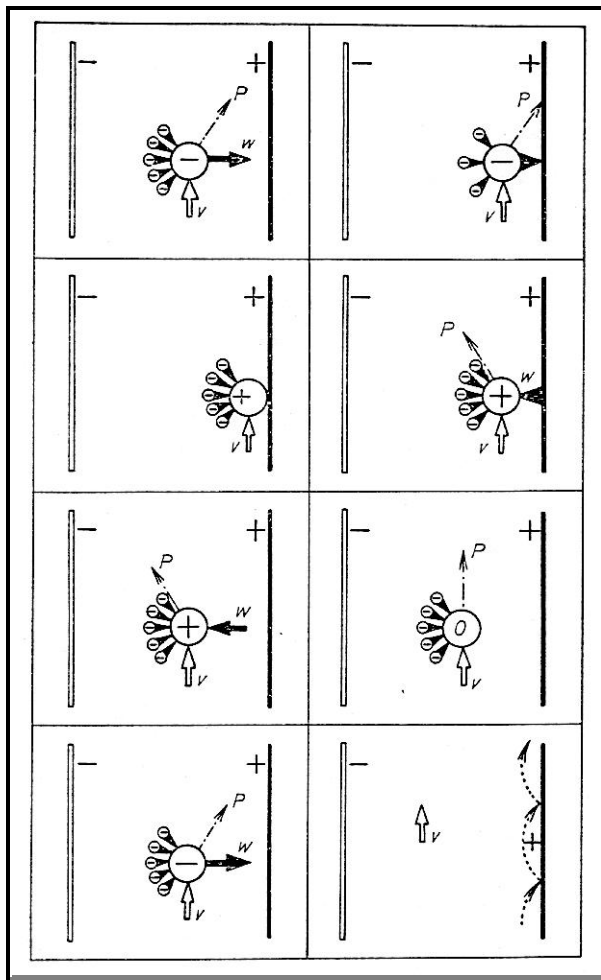
Figure 5.27　Repeated rebouncing of a conductive particle between two electrodes (picture from Böhm, 1982)

electrode wire as a result of high field strengths building up in the collected material layer. With very low resistivities ($< 10^4$ ohm.cm), usually as a result of presence of carbon, the particles will loose their charge very rapidly to, for example, water in the gas or other particles. Moreover, upon contact with the collection electrode or collected material layer they may rapidly switch sign (+ X -) and become re-entrained. This is illustrated by Figure 5.27 for a negatively charged particle.

Figure 5.26 shows also the large effect that the sulphur content of a fuel as coal has on fly ash resistivity. Part of the success of ESP has to do with the fact that its history lies at the east part of the US, where relatively high-sulphur coals are fired (*e.g.* Pittsburgh, Pocahontas, Illinois). Switching to low sulphur coals from the west part of the US (*e.g.* Powder River Basin) resulted in large problems with ESP performance, enforcing lower power outputs of coal-fired units. It was soon found that the small part of the fuel sulphur that is oxidised from SO_2 to SO_3 forms, with moisture, sulphuric acid (H_2SO_4) (**7** chapter 3) which condensates on the surface of the fly ash particles. This reduces the resistivity and increases the cohesivity of the dust (Scott, 1997). A lower fuel sulphur content leads to charging problems and more serious back-corona.

For coal fly ash conditions that may be difficult for proper ESP operation are shown in Figure 5.28, with options for improvement in Figure 5.29. Apart from sulphur (S), components that decrease fly ash resistivity are iron (Fe_2O_3,) sodium (Na_2O), and water. Components that increase resistivity, making precipitation more difficult are calcium (CaO), magnesium (MgO) silicon (SiO_2) and aluminum (Al_2O_3) (Soud, 1995).

- Operation near maximum resistivity
  (temperature approximately 150–190°C)

- Critical bulk resistivity for incipient back corona
  Cold-side ESP 1-3×10^{10} ohm cm
  Hot-side ESP 2-5×10^{9} ohm cm

- Bituminous coal ash
Sulphur	Low	$\leq 1\%$
$SiO_2 + Al_2O_3$	High	$>80\%$
Fe_2O_3	Low	$<5\%$
Na_2O	Low	$<0.5\%$

- Lignite ash
Sulphur	Low	$\leq 1\%$
$CaO + MgO > Fe_2O_3$	By 3-6 times	
Na_2O	Low	$<0.5\%$
Free lime	Available	

- Low gas moisture   5-7% volume

- Boiler fouling – loss of Na_2O with lignitic ash and hot-side ESP

Figure 5.28   Difficult conditions for ESP operation (from Carpenter, 1998)

- Flue gas conditioning
  (to lower fly ash resistivity)
- Pulse energisation
  (allows more useful power to be applied to the ESP)
- Humidification
  (spraying water into the flue gas to lower its temperature and reduce fly ash resistivity and cohesivity)
- Optimising existing surface
- Mechanical upgrades
  (such as increasing the specific collection area by adding additional fields or increasing the plate height, if space limitations allow)

Figure 5.29   Options for ESP performance inprovement (from Carpenter, 1998)

Table 5.10   Optimisation of an ESP after switch to lower sulphur fuel *(from Carpenter, 1998)*

Coal type	HHV, MJ/kg	Ash, wt%	Sulphur, wt%	ESP specific collection area, $m^{-1}s$
Midwestern bituminous	24.4	15	3.2	54
Switch to PRB	18.9	15	0.3	169
with pulse modulation				77
with SO_3 conditioning				59

How optimisation of an ESP can influence the performance after a fuel switch to a lower sulphur coal is given in Table 5.10. The performance of the ESP is expressed as specific collection area, SCA (= collection area/gas flow rate, unit: m²/(m³/s)) needed for a certain dust removal efficiency. Typically, switching from a 1%-wt sulphur coal to a 0.6 %-wt sulphur coal will require a 20% larger ESP collection area.

A very important property of the gas phase when it comes to particle resistivity is the moisture content of the gas, especially at temperatures below 200 EC. As Figure 5.30 shows (for cement kiln dust), a typical water content of ~10% in the gas can lower particle resistivity by several orders of magnitude. Water molecules are very active in removing electric charge from particles, and moisture plays an important role via its interaction with the sulphur oxides in the gas.

By its effect on the particle charge that is acquired, the resistivity of the particles or droplets determines the electric drift velocity the particle as illustrated by Figure 5.31. This translates to removal efficiency via the Deutsch equation.
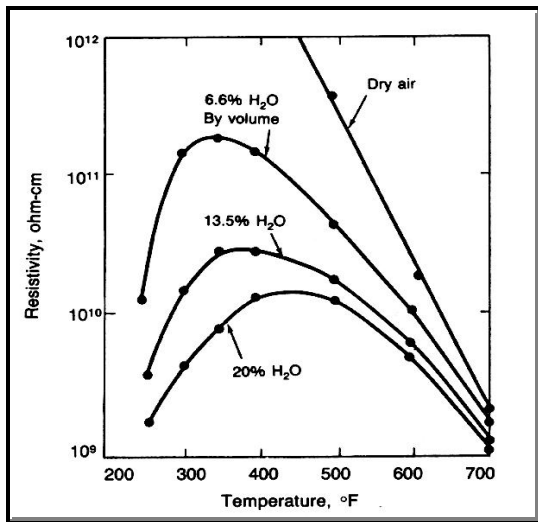
Figure 5.30 Effect of moisture on particle resistivity (picture from Cooper and Alley, 1994) (300EF = 149EC, 600EF = 316EC)
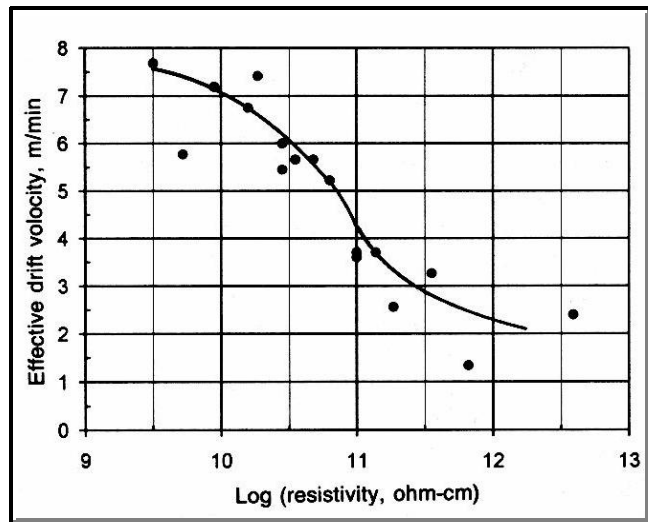
Figure 5.31 Typical relation between fly ash resistivity and electric drift velocity (picture from Cooper and Alley, 1994)

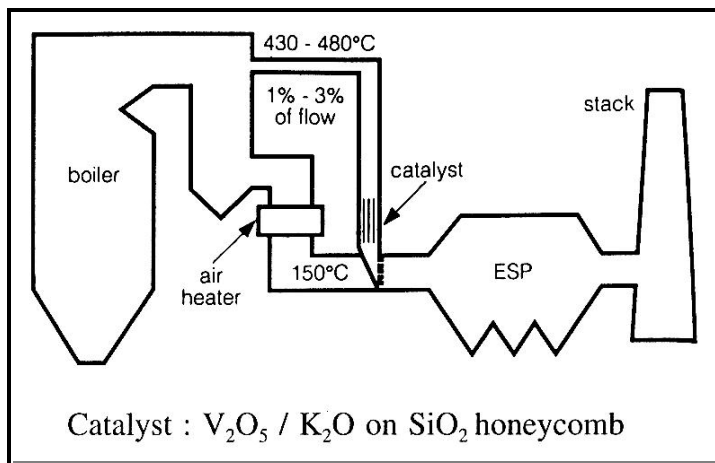## 5.7.8 ESP efficiency improvement, flue gas conditioning

Catalyst : V_2O_5 / K_2O on SiO_2 honeycomb

Figure 5.32 EPRICON SO_2 to SO_3 process for ESP (picture from Soud, 1995)

An ESP performance improvement process patented by EPRI is the EPRICON SO_2 to SO_3 converter process. A small part of the flue gas (with typically a few 1000 ppm SO_2 and some 10 ppm SO_3) is passed over a catalyst bed where a few % of the SO_2 in the flue gas is oxidised to SO_3 - see Figure 5.32. This reduces fly ash surface resistivity and improves efficiency as described above.

Another method is based on sulphur burning: if the fuel doesn't produce SO_2, elemental sulphur or SO_3 can be used for "conditioning" of the flue gas (actually the fly ash particles are being "conditioned"). Also combined injection of SO_3 and NH_3 can be employed, the first to adjust fly ash resistivity, the second to improve cohesivity and the effectivity of the ESP voltage. The cheapest option is to burn elemental sulphur in presence of a catalyst and injecting SO_3 into the flue gas. (Soud, 1995).

5.7.9 ESP design characteristics, hot/cold - side ESP, wet ESP.

Typical design data for ESPs are given in Table 5.11. Most ESPs are operated as so-called "cold-side" ESPs, located between air pre-heater and FGD system (if that is present) at 120-200EC. This is not optimal when considering fly ash resistivity (see Figure 5.26). Alternatively, so-called "hot-side" ESPs are operated at 300-450EC, upstream of the air pre-heater. Since particle resistivity is determined by volume conductivity under these conditions, there is less sensitivity to gas composition. A disadvantage is that heat losses from hot ESPs can be significant, and they are more sensitive to temperature changes when operating the furnace or boiler at partial load.

Table 5.11   Typical design characteristics for cold-side ESPs
(data from Cooper and Alley, 1994)

Temperature	120 - 200°C	Power / collector area	
Gas flow velocity	1 - 3 m/s	ash resistivity 10^4-10^7 ohm.cm	~ 43 W/m^2
Gas flow / collector area	15 - 125 s/m	ash resistivity 10^7 - 10^8 ohm.cm	~ 32 W/m^2
Plate-to-plate distance	0.15 - 0.4 m	ash resistivity 10^9-10^{10} ohm.cm	~ 27 W/m^2
Electric drift velocity	0.02 - 2 m/s	ash resistivity ~10^{11} ohm.cm	~ 22 W/m^2
Corona current / collector area	50 - 750μA/m^2	ash resistivity ~10^{12} ohm.cm	~ 16 W/m^2
Corona current / gas flow	0.05 - 0.3 J/m^3	ash resistivity ~10^{13} ohm.cm	~ 11 W/m^2

When an SCR unit for NOx control (**7** chapter 4) is part of the flue gas clean-up system (which operates at 350-400EC) it is beneficial to have the ESP upstream of the SCR. This "hot side, low dust" operation will improve SCR catalyst lifetime and reduce SCR operation and maintenance problems. Especially for flue gas from waste incineration furnaces this arrangement is preferable.

An interesting option that gives very high ESP efficiencies is to operate in a "wet" mode, *i.e.* with a stream of water that continuously removes the dust from the collector surfaces as a slurry. This finds application especially in Japan where ESPs located near cities are forced to control particulate emissions to 10 mg/m³$_{STP}$ or below. Advantages are high efficiency (less re-entrainment) and less sensitivity to particle resistivity, higher gas velocities (giving smaller devices) and that sub-micron particles can be collected as well. A major advantage is the absence of the rapping devices that are required to remove the particles from cold-side ESP collector surface. Disadvantages are that the gas temperature has to be reduced significantly, that corrosion problems can arise and that high dust and high SO_3 concentrations cause problems. Besides that, a waste water stream is generated that needs handling (Scott, 1997).

High temperature ESPs will be discussed further in section 5.11, below.